Leukemia Research 87 (2019) 106229

Contents lists available at ScienceDirect

Leukemia Research

journal homepage: www.elsevier.com/locate/leukres

Research paper

Gene expression profiling by mRNA sequencing reveals dysregulation of core genes in Rictor deficient T-ALL mouse model

Chunlan Hua[a], Xiangyu Chen[c], Weiping Yuan[b], Yang Li[a], Jing Yu[a], Haijun Li[a], Liang Ming[a,*]

[a] Department of Clinical Laboratory, The First Affiliated Hospital of Zhengzhou University, Zhengzhou, Henan, 450052, China
[b] State Key Laboratory of Experimental Hematology, Institute of Hematology and Blood Diseases Hospital, Center for Stem Cell Medicine, Chinese Academy of Medical Sciences and Peking Union Medical College, Tianjin 300020, China
[c] Department of Gastroenterology, The First Affiliated Hospital of Zhengzhou University, Zhengzhou, Henan, 450052, China

ARTICLE INFO

Keywords:
T-cell acute lymphoblastic leukemia
Rictor
mTOR
mRNA sequence
Gene expression profile

ABSTRACT

T-cell acute lymphoblastic leukemia (T-ALL) is a neoplastic disorder with peak incidence in children and young adults. The mTOR complex is an important component of the PI3K/Akt/mTOR signaling cascade and holds great promise for the treatment of hematopoietic malignancies. Previous studies have shown that the depression of Rictor, one of the components of the mTOR complex, prevents myeloproliferative disorders and leukemia However, knowledge of the progression of mTOR has not greatly improved the prognosis of T-ALL. To identify potential prognostic biomarkers for T-ALL, a whole-genome expression profile of Rictior deficient T-ALL mice was performed. As a result, 1475 differentially expressed genes (DEGs) were identified. Network analysis revealed 46 genes with a high network degree and fold-change value. Kaplan-Meier analysis identified ten crucial genes which significantly associated with survival in Rictor deficient T-ALL mice. These findings provide potential therapeutic targets in leukemia and bear immediate relevance to patients with leukemia.

1. Introduction

T-cell acute lymphoblastic leukemia (T-ALL), a neoplastic disorder with peak incidence in children and young adults, accounts for approximately 25% of adult ALL and 10–15% of pediatric ALL [1–4]. Although the outcome of T-ALL patients has significantly improved with the advance of therapies in recent years, the long-term survival rate of adult T-ALL patients remains very poor, and the need to understand the molecular events occurring during T-ALL development is urgent [5,6]. Efforts to develop targeted molecules against deregulated signaling pathways that sustain T-ALL cell growth and survival should be made.

Mammalian target of rapamycin (mTOR) is an evolutionarily conserved kinase in eukaryotes that plays a critical role in regulating cell growth, proliferation, and survival [7,8]. mTOR forms two complexes: mTOR complex 1 (mTORC1) and 2 (mTORC2). mTORC1, which consists of mTOR (catalytic subunit), regulatory associated protein of mTOR (Raptor), DEP domain-containing mTOR-interacting protein (DEPTOR), mammalian lethal with SEC13 protein 8 (mLST8/GbL), and 40 kDa Pro-rich Akt substrate (PRAS40), is rapamycin sensitive [9,10]. Furthermore, mTOR controls cell growth and proliferation via the phosphorylation of multiple substrates, such as p70 ribosomal protein S6 Kinase (p70S6K) and eukaryote translation initiation factor 4E binding protein 1 (4E-BP1) [11]. mTORC2, which is formed by mTOR, rapamycin-insensitive companion of mTOR (Rictor), mLST8, mammalian stress-activated map kinase-interacting protein 1 (mSin1), protein observed with Rictor 1 (Protor-1), and Protor-2, is essential for Akt activity via the phosphorylation of Akt at the hydrophobic Ser473 site and is thought to be rapamycin insensitive [12,13]. Over the past few decades, the mTOR pathway has been shown to play key roles in human cancers. This pathway mainly relays signals from upstream receptors for activation and signals from downstream effectors to control gene expression [14]. Increasing attention has focused on mTOR mutations and the function of mTOR in the transmission of proliferative signals from outside of the membrane to inside of the membrane in hematopoietic malignancies.

The efforts of researchers and clinicians have advanced the understanding of T-ALL, including the fusion of the TCRβ locus and the 3' region of NOTCH1, which leads to overexpression of the activated form of NOTCH1 (ICN1). This mutation is generally observed during the molecular analysis of human T-ALL [15,16]. NOTCH controls the activity of mTOR signaling in leukemic T-cells through its direct transcriptional target c-myc, and the hyperactivation of mTOR signaling sustains T-ALL [17]. The growth of T-ALL patient samples can be

* Corresponding author.
E-mail address: mingliang3072@163.com (L. Ming).

https://doi.org/10.1016/j.leukres.2019.106229
Received 22 April 2019; Received in revised form 9 September 2019; Accepted 25 September 2019
Available online 26 September 2019

inhibited through cell cycle arrest and apoptosis by treatment with a dual mTOR pathway inhibitor [18]. mTOR activation in T-ALL is also blocked via the dephosphorylation of downstream targets of mTOR, including p70S6K and 4EBP [19,20]. Furthermore, dysregulation of mTORC2 deficiency in mice partially blocks thymocyte development at the double-negative 3 stage and thus affects T-cell lymphopoiesis [21].

Over the past decades, efforts have been made to maximize the chance of cure and pathogenesis of T-ALL through collaboration among clinicians, pathologists, and biologists. The crucial events leading to T-ALL transformation and development remain difficult to study. To date, no specific and accurate molecular markers for the early diagnosis and treatment of T-ALL have been established; therefore, further efforts to identify new molecular markers for T-ALL should be made.

In the present study, we sequenced mRNA from Rictor deficient T-ALL mice and control mice. Differentially expressed genes (DEGs) were identified and subjected to network analysis. We then performed a Kaplan-Meier analysis of core gene networks and identified several survival-associated genes that act as potential markers for the prognosis of patients with T-ALL.

2. Materials and methods

2.1. mRNA sequencing (mRNA-seq)

Rictor deficient T-ALL mouse model was established as in our previous experiment. T-ALL cells were sorted by a FACSAria III (BD Bioscience), and total RNA was extracted with TRIzol reagent (Invitrogen). Then, mRNA-seq was performed to profile mRNA expression levels in Rictor knockout T-ALL cells and control T-ALL cells. RNA-seq reads were aligned to the mouse genome reference sequence (GRCm38/mm10) using TopHat with a tolerance of two mismatches [22].

2.2. Differential expression analysis

After obtaining raw datasets from gene expression profiling by mRNA-seq, we performed differential expression testing with Cuffdiff to detect DEGs. The t-test and false discovery rate (FDR) correction were used to test the significance of differences in gene expression between Rictor deficient T-ALL cells and control cells, and only those genes with adjusted $p < 0.05$ and $|\log2\text{fold change}| > 1$ (fold change > 2 or < 0.5) were considered to be significantly differentially expressed.

2.3. Functional enrichment analysis

To identify functions involved in DEGs in Rictor deficient T-ALL cells, the Database for Annotation, Visualization and Integrated Discovery (DAVID, david.ncifcrf.gov/) bioinformatics resource was used for functional enrichment analysis [23], and Gene Ontology (GO) terms and Kyoto Encyclopedia of Genes and Genome (KEGG) pathways with $p < 0.05$ were screened out.

2.4. Network analysis

The relationships between DEGs were determined according to protein-protein interaction (PPI) networks [24,25]. Pearson correlation coefficients (PCCs) for these relationships were calculated. Based on the significant relationships ($|\log PCC| > 0.75$), modular analysis of the PPI network was conducted using the MCODE plug-in of Cytoscape [26,27].

2.5. Kaplan-Meier analysis

Hub network genes (genes with high degree) are thought to play an important role in T-ALL progression, which accounts for the large number of genes that directly interact with hub network genes. In our present study, we conducted a Kaplan-Meier analysis of hub network genes with Gene Expression Profile Interactive Analysis (GEPIA, http://gepia.cancer-pku.cn/detail.php) to identify genes significantly associated with the overall survival (OS) of T-ALL.

2.6. RNA extraction and real-time PCR

Total RNA was extracted using the RNeasy Mini Kit according to the manufacturer's instructions (QIAGEN, Valencia, CA). Reverse transcription was performed using Oligo (dT)18, 2 × TS Reaction Mix, and TransScript RT/RI Enzyme Mix. Real-time PCR was performed using FastStart Universal SYBR Green Master (Rox), 0.4 mM of specific forward and reverse primers and normalized cDNA. The parameters for the thermal cycling of PCR were as follows: 15 s at 95°C and 60 s at 60°C for 45 cycles, The measured transcript copy numbers were normalized using GAPDH as a reference. The fold changes were calculated according to the ΔΔCT method. All primer sequences are listed in Table 3.

3. Results

3.1. Data quality and RNA sequences

mRNA-seq has broad applications across biomedical research. One of the key challenges of mRNA-seq is to ensure that sequences are of sufficiently high quality for downstream analysis, as the inclusion of compromised cells inevitably affects data interpretation. As shown in Fig. 1A, exon No. 3 of Rictor was completely knocked out. The high quality of the sequences is shown in Fig. 1B. Correlation plots of expression profiling for Rictor$^{-/-}$ and control groups in RNA-seq is shown in Fig. 1C, volcano plot of the genes is shown in Fig. 1D, the thresholds of log2fold change < -1 represent downregulated genes, log2fold change > 1 represent upregulated genes, and $|\log2\text{fold change}| \leq 1$ represent the non-differential expressed genes.

3.2. DEGs and functional enrichment analysis

With the thresholds of adjusted $p < 0.05$ and $|\log2\text{fold change}| > 1$, a total of 1475 DEGs between Rictor deficient T-ALL cells and control samples were identified; 959 of these DEGS were upregulated, and 516 were downregulated genes. The KEGG pathways significantly enriched in upregulated genes and downregulated genes were analyzed separately. As a result, upregulated genes were involved in 37 KEGG pathways associated with the phagosome; tuberculosis; transcriptional misregulation in cancer, including the Rap1 signaling pathway; and the MAPK signaling pathway (Fig. 2A). In addition, a total of 13 KEGG pathways associated with metabolism and cell adhesion, such as arginine and proline metabolism, Fc gamma R-mediated phagocytosis, cell adhesion molecules (CAMs), and the cAMP signaling pathway, were significantly enriched in downregulated genes (Fig. 2B). GO term enrichment analysis was performed for DEGs, and enrichment map of upregulated genes and downregulated genes are displayed in Fig. 2C and D. In the GO chord plot, genes are shown on the left, and different GO terms are shown on the right. Connections indicate the enrichment of different terms with different genes. For example, among the upregulated genes, IL2RβR, TGRβR2 and JUN were enriched in transcriptional misregulation in cancer, while among the downregulated genes, PYCR2, GOT1 and CKB were enriched in arginine and proline metabolism.

3.3. Network analysis

Combined analysis of the PPI network identified 3026 interactions pairs among the 1475 DEGs. Modular analysis identified a total of seven network modules, as shown in Fig. 3. In order to interpret the biological processes of every module, KEGG pathway analysis was conducted through the KOBAS.3 online tool (kobas.cbi.pku.edu.cn/) for genes in the modules [28]. As a result, in addition to KEGG pathways involved in

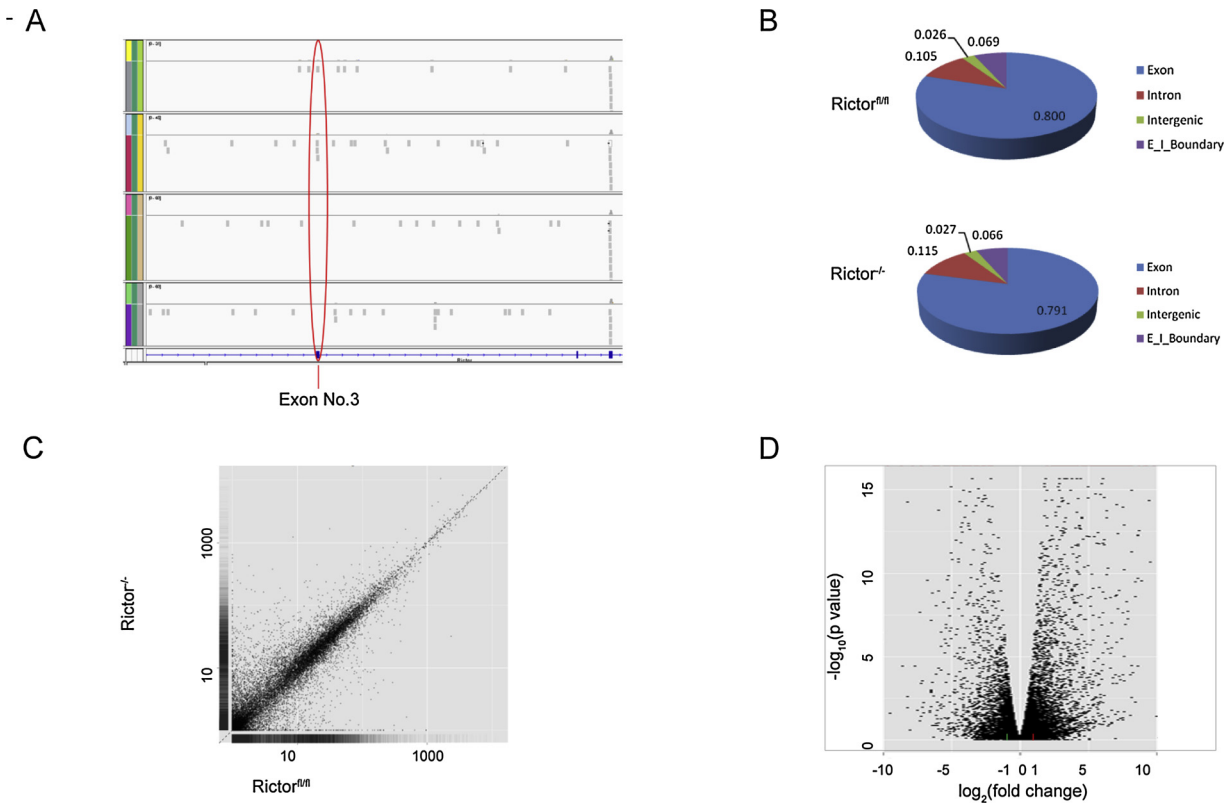

Fig. 1. (A) No reads mapped to exon No. 3 in Rictor$^{-/-}$ T-ALL cells. (B) Read distribution showing most reads mapped to exon regions. Global visualization of the expression profile of the T-ALL model: Correlation plots of expression profiling for Rictor$^{-/-}$ and control groups in RNA-seq is shown (C), volcano plot of the genes (D), X and Y axis is log2fold change and –log10-based adjusted p value. the threshold of log2fold change < -1 represent downregulated genes, log2fold change > 1 represent upregulated genes, and |log2fold change| ≤ 1 represent the non-differential expressed genes.

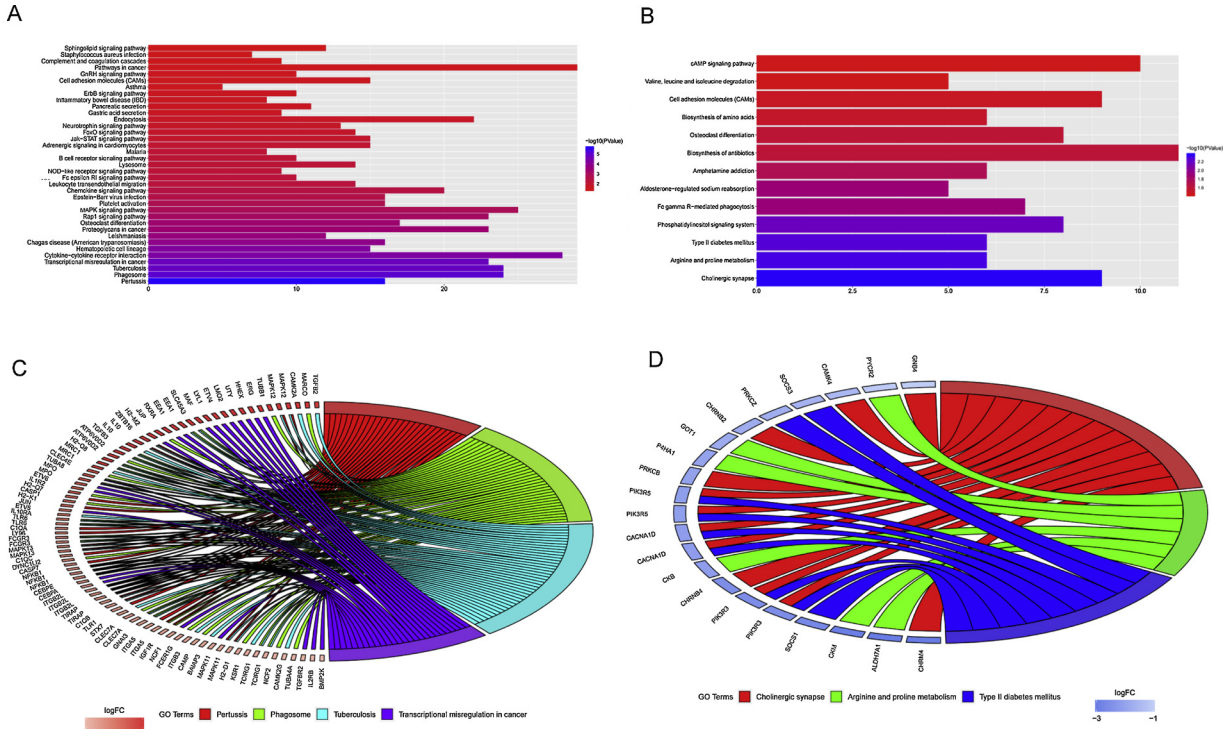

Fig. 2. Signaling pathways significantly enriched in upregulated genes (A) and downregulated genes (B). The vertical axis is the gene number in the corresponding signaling pathway. The x-axis shows the –log10-transformed expected p value, The color of the bar indicates significance, with darker (blue) shades indicating the smaller p value. GO term enrichment analysis was performed for DEGs, and an enrichment map of upregulated genes (C) and downregulated genes (D) is shown. (For interpretation of the references to colour in this figure legend, the reader is referred to the web version of this article).

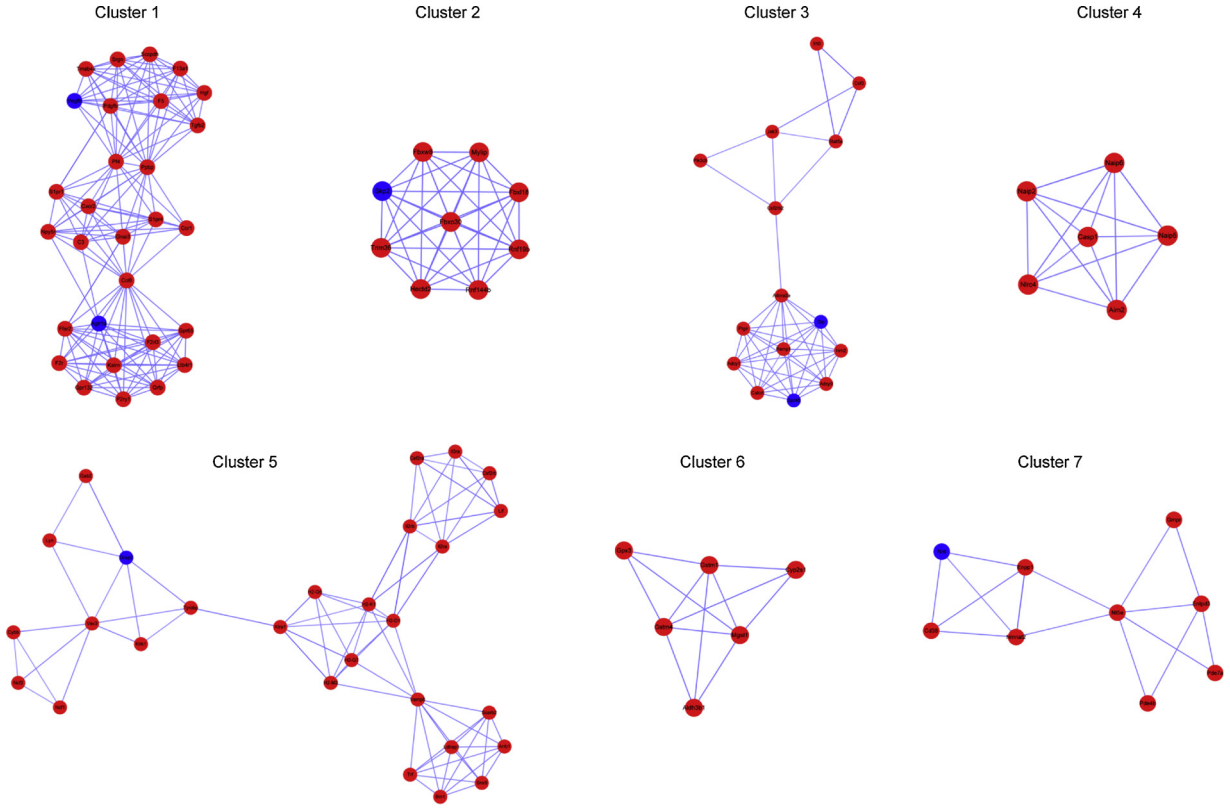

Fig. 3. Modular network analysis. Nodes and edges represent genes and interactions among genes, respectively. Blue and red colors indicate downregulation and upregulation, respectively. (For interpretation of the references to colour in this figure legend, the reader is referred to the web version of this article).

cancer, KEGG pathways associated with other cellular functions, such as cytokine-cytokine receptor interactions, endocytosis and the phagosome, were also significantly enriched in network modules (Table 1).

3.4. Kaplan-Meier analysis

To identify potential biomarkers involved in T-ALL progression, genes with a network degree > 10 (genes that directly interact with ≥10 other genes in the network) and a |log2fold change| > 2 were screened. As a result, 46 genes, all of which were upregulated, were identified (Table 2). Kaplan-Meier analysis of the 46 genes based on the GEPIA dataset identified ten genes (HGF, IL2RA, IL10, KALRN, P2RY1, PF4, PIK3CB, PPBP, QRFP, and SCCPDH) significantly associated with T-ALL survival (Fig. 4). These results demonstrate that the expression of HGF, PIK3CB, QRFP and SCCPDH in T-ALL samples is negatively associated with the survival rates of T-ALL mice; however, the expression of PPBP, IL2RA, IL10, KALRN, P2YRY1, and PF4 is positively associated with the survival rates of T-ALL mice. We peformed correlation analysis to identify the associations of these genes with Rictor (Pearson correlation coefficient and p value) according to GEPIA, as a result, three genes, IL2RA, P2RY1 and PIK3CB, have a close relationship with Rictor (Fig. 5); these genes should serve as valuable treatment biomarkers for T-ALL.

3.5. RT-PCR analysis

Expression differences of HGF, IL2RA, IL10, KALRN, P2RY1, PF4, PIK3CB, PPBP, QRFP, and SCCPDH between Rictor deficient T-ALL cells and control T-ALL cells were investigated using RT-PCR for their significant associations with T-ALL mice's OS. All of these genes were upregulated in the Rictor deficient T-ALL samples compared to their levels in control samples, which were consistent with results from the RNA-seq analysis (Fig. 6).

4. Discussion

T-ALL is a highly heterogeneous group of malignant diseases characterized by changes in gene expression caused by histone modifications, hypermethylation of tumor suppressor genes and miRNA and lncRNA abnormalities [29]. T-ALL is initiated by the disorder of some crucial biological processes, such as differentiation, self-renewal capacity, proliferation and apoptosis [30]. T-ALL accounts for 25% of adult ALL and 10–15% of childhood ALL. Despite the significant improvement in the survival rate of T-ALL patients with therapeutic advancements, the long-term outcome in adult patients with relapsed T-ALL remains poor [31,32]. The relapse may reflect a failure to eliminate leukemia stem cells (LSCs) that retain the ability for self-renewal and differentiation [33]. LSCs have been extensively investigated and well documented in acute myeloid leukemia [34]. The existence of LSCs in T-ALL is still controversial. However, the cure rate of T-ALL could be notably improved by the identification of molecular markers to aid the effective early diagnosis. In our studies, we identified 1475 DEGs by gene expression dataset analysis and constructed a disease network by using these DEGs. Finally, we determined seven T-ALL-associated disease clusters. Survival analysis identified ten genes significantly associated with the survival rate of mice with T-ALL.

The mTOR signaling pathway is crucial to many widely divergent physiological processes [35]. Previous studies have demonstrated that this signaling cascade is deregulated in hematopoietic malignancies and contributes to the pathogenesis and therapy in ALL [36]. Extensive research on the mTOR pathway within the last few years bring a couple of improvements in our understanding of the complex network of regulatory loops in hematopoietic malignancies, making targeting the mTOR pathway a potential therapeutic approach in clinical trials. The conditional deletion of Rictor, an essential component of mTORC2, impaired the activation of mTORC2 and retarded ALL development in leukemic mice [1–48]. In this study, GO term enrichment and clustering

Table 1
Significantly enriched KEGG pathways of the seven clusters.

Cluster 1			
#Term	ID	P-Value	FDR
Cytokine-cytokine receptor interaction	mmu04060	3.47E-13	2.85E-11
Neuroactive ligand-receptor interaction	mmu04080	3.67E-11	1.51E-09
Rap1 signaling pathway	mmu04015	2.61E-10	7.13E-09
Pathways in cancer	mmu05200	4.85E-10	9.95E-09
Complement and coagulation cascades	mmu04610	7.72E-09	1.17E-07
Chemokine signaling pathway	mmu04062	8.56E-09	1.17E-07
Platelet activation	mmu04611	2.47E-06	2.89E-05
Phospholipase D signaling pathway	mmu04072	4.78E-06	4.90E-05
Renal cell carcinoma	mmu05211	2.09E-05	0.0001904
AGE-RAGE signaling pathway in diabetic complications	mmu04933	6.93E-05	0.000531274
Chagas disease (American trypanosomiasis)	mmu05142	7.13E-05	0.000531274
Sphingolipid signaling pathway	mmu04071	0.000121286	0.00082879
PI3K-Akt signaling pathway	mmu04151	0.000136485	0.000860906
FoxO signaling pathway	mmu04068	0.000151489	0.000887292
cAMP signaling pathway	mmu04024	0.000456626	0.002496221
Focal adhesion	mmu04510	0.000490502	0.002513823
Regulation of actin cytoskeleton	mmu04810	0.000601692	0.00290228
Malaria	mmu05144	0.000702526	0.003064771
Ras signaling pathway	mmu04014	0.00071013	0.003064771
Leishmaniasis	mmu05140	0.00123316	0.005050034
Endocytosis	mmu04144	0.001410607	0.005050034
Melanoma	mmu05218	0.001416473	0.005050034
Renin secretion	mmu04924	0.001416473	0.005050034
Pertussis	mmu05133	0.001493226	0.005101856
EGFR tyrosine kinase inhibitor resistance	mmu01521	0.001819686	0.00596857
Gap junction	mmu04540	0.001994506	0.006290366
Cluster 2			
#Term	ID	P-Value	FDR
Ubiquitin mediated proteolysis	mmu04120	0.000507548	0.004567931
Small cell lung cancer	mmu05222	0.019836858	0.062790754
Cell cycle	mmu04110	0.02894353	0.062790754
FoxO signaling pathway	mmu04068	0.031208413	0.062790754
mTOR signaling pathway	mmu04150	0.035949389	0.062790754
Cluster 3			
#Term	ID	P-Value	FDR
Vascular smooth muscle contraction	mmu04270	7.53E-12	9.18E-10
Jak-STAT signaling pathway	mmu04630	2.87E-11	1.75E-09
HTLV-I infection	mmu05166	7.65E-08	3.11E-06
Platelet activation	mmu04611	1.47E-07	4.48E-06
Calcium signaling pathway	mmu04020	6.78E-07	1.64E-05
Chemokine signaling pathway	mmu04062	9.42E-07	1.64E-05
cAMP signaling pathway	mmu04024	9.42E-07	1.64E-05
Rap1 signaling pathway	mmu04015	1.30E-06	1.98E-05
Regulation of lipolysis in adipocytes	mmu04923	1.59E-06	2.16E-05
Longevity regulating pathway – multiple species	mmu04213	2.23E-06	2.72E-05
Gastric acid secretion	mmu04971	3.26E-06	3.62E-05
Neuroactive ligand-receptor interaction	mmu04080	3.90E-06	3.97E-05
Insulin secretion	mmu04911	5.25E-06	4.93E-05
Progesterone-mediated oocyte maturation	mmu04914	5.99E-06	5.22E-05
Endocrine resistance	mmu01522	7.02E-06	5.51E-05
Longevity regulating pathway	mmu04211	7.23E-06	5.51E-05
Estrogen signaling pathway	mmu04915	7.68E-06	5.51E-05
Chagas disease (American trypanosomiasis)	mmu05142	9.14E-06	6.19E-05
Amoebiasis	mmu05146	1.11E-05	7.10E-05
Cholinergic synapse	mmu04725	1.16E-05	7.10E-05

Table 1 (*continued*)

Cluster 3			
#Term	ID	P-Value	FDR
Pathways in cancer	mmu05200	1.43E-05	8.32E-05
Inflammatory mediator regulation of TRP channels	mmu04750	1.60E-05	8.88E-05
Measles	mmu05162	2.13E-05	0.000113162
Phospholipase D signaling pathway	mmu04072	2.46E-05	0.00012521
Adrenergic signaling in cardiomyocytes	mmu04261	2.77E-05	0.000135232
Oxytocin signaling pathway	mmu04921	3.10E-05	0.000145626
cGMP-PKG signaling pathway	mmu04022	4.05E-05	0.000182848
Epstein-Barr virus infection	mmu05169	9.54E-05	0.000415782
Viral carcinogenesis	mmu05203	0.00011189	0.000470711
Cytokine-cytokine receptor interaction	mmu04060	0.000140674	0.000572073
Malaria	mmu05144	0.000184022	0.000724214
Acute myeloid leukemia	mmu05221	0.00023708	0.000903867
Ovarian steroidogenesis	mmu04913	0.0002452	0.000906497
PI3K-Akt signaling pathway	mmu04151	0.000316014	0.001133933
Thyroid hormone synthesis	mmu04918	0.000363001	0.001230171
Bile secretion	mmu04976	0.000363001	0.001230171
Chronic myeloid leukemia	mmu05220	0.000383135	0.001263026
Prolactin signaling pathway	mmu04917	0.000393401	0.001263026
Salivary secretion	mmu04970	0.000435802	0.001363278
Gap junction	mmu04540	0.000526982	0.001560924
Aldosterone synthesis and secretion	mmu04925	0.000526982	0.001560924
ErbB signaling pathway	mmu04012	0.000538976	0.001560924
GnRH signaling pathway	mmu04912	0.000551102	0.001560924
GABAergic synapse	mmu04727	0.00056336	0.001560924
Dilated cardiomyopathy	mmu05414	0.000575751	0.001560924
Morphine addiction	mmu05032	0.000613712	0.001627672
Circadian entrainment	mmu04713	0.000679614	0.001761854
Melanogenesis	mmu04916	0.000693189	0.001761854
AGE-RAGE signaling pathway in diabetic complications	mmu04933	0.000748796	0.001791238
Pancreatic secretion	mmu04972	0.000748796	0.001791238
Retrograde endocannabinoid signaling	mmu04723	0.000748796	0.001791238
T cell receptor signaling pathway	mmu04660	0.000777385	0.001823865
Toxoplasmosis	mmu05145	0.000896957	0.002064693
Glutamatergic synapse	mmu04724	0.00092815	0.002093834
Oocyte meiosis	mmu04114	0.000943941	0.002093834
FoxO signaling pathway	mmu04068	0.001268498	0.002763513
Apoptosis	mmu04210	0.00134273	0.002864069
Signaling pathways regulating pluripotency of stem cells	mmu04550	0.001361607	0.002864069
Hepatitis B	mmu05161	0.001477543	0.003055258
Purine metabolism	mmu00230	0.002196369	0.00446595
Cluster 4			
#Term	ID	P-Value	FDR
Legionellosis	mmu05134	5.84E-14	2.22E-13
NOD-like receptor signaling pathway	mmu04621	6.34E-14	2.22E-13
Cytosolic DNA-sensing pathway	mmu04623	4.28E-05	9.99E-05
Salmonella infection	mmu05132	6.30E-05	0.000110327
Amyotrophic lateral sclerosis (ALS)	mmu05014	0.008194987	0.011472981
Pertussis	mmu05133	0.011580202	0.013510236
Influenza A	mmu05164	0.026543063	0.026543063
Cluster 5			
#Term	ID	P-Value	FDR
Endocytosis	mmu04144	8.94E-15	4.56E-13
Phagosome	mmu04145	1.26E-12	3.21E-11
Graft-versus-host disease	mmu05332	2.00E-11	3.41E-10
Natural killer cell mediated cytotoxicity	mmu04650	3.94E-10	5.02E-09
HTLV-I infection	mmu05166	1.69E-09	1.73E-08
Jak-STAT signaling pathway	mmu04630	2.06E-09	1.75E-08
Allograft rejection	mmu05330	2.59E-09	1.89E-08
Type I diabetes mellitus	mmu04940	3.57E-09	2.28E-08
Autoimmune thyroid disease	mmu05320	6.40E-09	3.63E-08

(*continued on next page*)

Table 1 (*continued*)

Cluster 5			
#Term	ID	P-Value	FDR
Fc gamma R-mediated phagocytosis	mmu04666	7.53E-09	3.84E-08
Viral myocarditis	mmu05416	1.03E-08	4.76E-08
Antigen processing and presentation	mmu04612	1.13E-08	4.82E-08
Epstein-Barr virus infection	mmu05169	1.71E-08	6.71E-08
Viral carcinogenesis	mmu05203	2.35E-08	8.54E-08
Cytokine-cytokine receptor interaction	mmu04060	3.70E-08	1.26E-07
Osteoclast differentiation	mmu04380	4.93E-08	1.57E-07
Cell adhesion molecules (CAMs)	mmu04514	1.91E-07	5.72E-07
Herpes simplex infection	mmu05168	6.11E-07	1.73E-06
Leukocyte transendothelial migration	mmu04670	2.00E-06	5.37E-06
Chemokine signaling pathway	mmu04062	1.34E-05	3.41E-05
Fc epsilon RI signaling pathway	mmu04664	1.96E-05	4.75E-05
Hematopoietic cell lineage	mmu04640	3.82E-05	8.86E-05
Leishmaniasis	mmu05140	0.001149495	0.002548881
B cell receptor signaling pathway	mmu04662	0.001428568	0.003035707
PI3K-Akt signaling pathway	mmu04151	0.002082028	0.004247337
T cell receptor signaling pathway	mmu04660	0.002731919	0.005358765
HIF-1 signaling pathway	mmu04066	0.002987791	0.005643604
Platelet activation	mmu04611	0.003703583	0.006745812
Measles	mmu05162	0.004683163	0.007961377
Apoptosis	mmu04210	0.004683163	0.007961377
SNARE interactions in vesicular transport	mmu04130	0.0243208	0.040011639
Cluster 6			
#Term	ID	P-Value	FDR
Metabolism of xenobiotics by cytochrome P450	mmu00980	1.01E-13	1.41E-12
Glutathione metabolism	mmu00480	8.38E-11	5.87E-10
Drug metabolism - cytochrome P450	mmu00982	1.56E-10	7.28E-10
Chemical carcinogenesis	mmu05204	5.56E-10	1.94E-09
Platinum drug resistance	mmu01524	1.76E-07	4.93E-07
Phenylalanine metabolism	mmu00360	0.003872562	0.008363653
Histidine metabolism	mmu00340	0.004181826	0.008363653
beta-Alanine metabolism	mmu00410	0.005263621	0.009211337
Tyrosine metabolism	mmu00350	0.006344437	0.009869124
Glycolysis / Gluconeogenesis	mmu00010	0.010350331	0.014151645
Thyroid hormone synthesis	mmu04918	0.01111915	0.014151645
Retinol metabolism	mmu00830	0.013882779	0.015115827
Arachidonic acid metabolism	mmu00590	0.014036125	0.015115827
Metabolic pathways	mmu01100	0.015476538	0.015476538
Cluster 7			
#Term	ID	P-Value	FDR
Nicotinate and nicotinamide metabolism	mmu00760	1.15E-13	1.60E-12
Purine metabolism	mmu00230	9.16E-13	6.41E-12
Metabolic pathways	mmu01100	4.85E-06	2.26E-05
Morphine addiction	mmu05032	0.000212513	0.000740645
Pyrimidine metabolism	mmu00240	0.000264516	0.000740645
Epstein-Barr virus infection	mmu05169	0.001275897	0.002977093
Pantothenate and CoA biosynthesis	mmu00770	0.00441301	0.00882602
Starch and sucrose metabolism	mmu00500	0.012727055	0.022272347
Salivary secretion	mmu04970	0.018235409	0.028366192
Hematopoietic cell lineage	mmu04640	0.020293988	0.028411583
Pancreatic secretion	mmu04972	0.023944212	0.030474452
Oxytocin signaling pathway	mmu04921	0.036399833	0.042466472
Calcium signaling pathway	mmu04020	0.04179059	0.04500525

analysis were conducted for the 1475 DEGs, and the GO terms were divided into seven groups according to their biological roles in cellular metabolism. Among the seven groups, five are involved in cell proliferation, apoptosis, and metabolism, and these cellular activities are closely associated with the mTOR signaling pathway. Therefore, the seven GO term groups identified in the present study represent typical

Table 2
46 DEGs with degree > = 10 and $|\log_2(\text{Fold Change})| > 2$.

Gene Symbol	Full name	logFC	Degree
F5	coagulation factor V	2.00314	11
TMSβ4	thymosin, beta 4, X chromosome	2.0082	10
	hepatocyte growth factor	2.09449	10
S1PR4	sphingosine-1-phosphate receptor 4	2.11317	19
CSF2R β2	colony stimulating factor 2 receptor, beta 2, low-affinity (granulocyte-macrophage)	2.12149	18
P1CG2	phospholipase C, gamma 2	2.2054	11
GPR65	G-protein coupled receptor 65	2.25482	10
CCL6	chemokine (C-C motif) ligand 6	2.28213	34
JUN	jun proto-oncogene	2.3267	11
H2-K1	histocompatibility 2, K1, K region	2.34485	12
STAT5A	signal transducer and activator of transcription 5A	2.43355	21
RHOJ	ras homolog family member J	2.49945	22
C3	complement component 3	2.59929	15
SRGN	serglycin	2.62445	11
PDGFB	platelet derived growth factor, B polypeptide	2.79121	25
MBOAT4	membrane bound O-acyltransferase domain containing 4	2.83803	12
QRFP	pyroglutamylated RFamide peptide	2.94032	12
RHOQ	ras homolog family member Q	2.98723	14
LIF	leukemia inhibitory factor	2.99491	13
F2R	coagulation factor II (thrombin) receptor	3.18189	16
SCCPDH	saccharopine dehydrogenase (putative)	3.19699	19
ERBB3	erb-b2 receptor tyrosine kinase 3	3.26851	10
PF4	platelet factor 4	3.39455	12
S1PR1	sphingosine-1-phosphate receptor 1	3.39779	30
IL10	interleukin 10	3.43832	11
DCN	decorin	3.47454	14
VAMP8	vesicle-associated membrane protein 8	3.47658	15
ENTPD3	ectonucleoside triphosphate diphosphohydrolase 3	3.54615	12
ADCY1	adenylate cyclase 1	3.61683	19
ARRβ1	arrestin, beta 1	3.6206	12
KALRN	kalirin, RhoGEF kinase	3.62664	17
JUP	junction plakoglobin	3.73658	13
PIK3Cβ	phosphatidylinositol-4,5-bisphosphate 3-kinase catalytic subunit beta	3.76802	11
PPBP	pro-platelet basic protein	3.8706	14
CTNNα1	catenin (cadherin associated protein), alpha 1	4.15962	20
VAV3	vav 3 oncogene	4.22265	22
DECR1	2,4-dienoyl CoA reductase 1, mitochondrial	4.34263	24
P2RY1	purinergic receptor P2Y, G-protein coupled 1	4.56938	10
ERBB2	erb-b2 receptor tyrosine kinase 2	5.93132	13
CSF3	colony stimulating factor 3 (granulocyte)	5.93413	19
MAPK12	mitogen-activated protein kinase 12	6.21521	10
KIT	KIT proto-oncogene receptor tyrosine kinase	6.41572	15
RHOD	ras homolog family member D	6.44247	10
IL2Rα	interleukin 2 receptor, alpha chain	7.86016	16
TGFβ2	transforming growth factor, beta 2	8.91502	28
DGFRβ	platelet derived growth factor receptor, beta polypeptide	8.14538	12

biological processes associated with the progression of T-ALL.

After we identified the 1475 DEGs, a T-ALL network was constructed, and seven disease clusters were ultimately identified. Several cancer-associated signaling pathways and metabolic processes were observed by enrichment analysis of the DEGs in each cluster. The PI3K/Akt signaling pathway was significantly enriched in the DEGs in cluster 1, cluster 3 and cluster 5, and the FoxO signaling pathway, which is closely associated with tumor progression, was significantly enriched in the DEGs in cluster 1, cluster 2 and cluster 3. Activation of the PI3K/Akt pathway is a common feature in myeloid and lymphoid leukemic cells [38]. Rictor/mTORC2 deficiency affects the activation of Akt by suppressing the phosphorylation of Akt at S473 [39]. FoxOs are tumor suppressors that regulate cell differentiation, metabolism and apoptosis

Table 3
RT-PCR primer sequence.

Primer		Sequence (5'-3')
HGF	Forward	CATTGGTAAAGGAGGCAGCTATAAA
	Reverse	GGATTTCGACAGTAGTTTTCCTGTAGG
IL2RA	Forward	ATGGAGCCACGCTTGCTGATGTTG
	Reverse	CCATTGTGAGCACAA ATGTCTCCG
IL10	Forward	GCACTGCTATGCTGCCTGCTCTTACTG
	Reverse	ATGGCCTTGTAGACACCTTGGTCTTGG
KALRN	Forward	CCGACTCTTGGACTACCTTATGA
	Reverse	CGACCCTACAGTTGTGCAG
P2RY1	Forward	TGGCACAAGGCGTCTAACTAT
	Reverse	GACTTCCTCTTGACGGAGGTG
PF4	Forward	CCGAAGAAAGCGATGGAGATCT
	Reverse	CCAGGCAAATTTTCCTCCCA
PIK3CB	Forward	CTATGGCAGACAACCTTGACAT
	Reverse	CAGAAGGAAATCGACGGATATGG
PPBP	Forward	CTCAGACCTACATCGTCCTGC
	Reverse	GTGGCTATCACTTCCACATCAG
QRFP	Forward	GAAGGGGACCCACAGACATC
	Reverse	TCTTGCCTCCCTAGACGGAAG
SCCPDH	Forward	AGTAATCCAGCCTCACTTGATGA
	Reverse	AGGTTCCCCACAGATGTCAATA

through integrating signals from multiple signaling pathways, including the PI3K/Akt pathway. Akt mediates the phosphorylation of FoxOs and leads to their nuclear exclusion and subsequent inactivation [40]. previous studies demonstrated that inactivation of mTORC2 caused the overexpression of FoxO3a and its downstream effectors and eased the progression of NOTCH-induced T-ALL and chronic myeloid leukemia [41,42].

Survival analysis revealed ten DEGs that are significantly associated with the survival rates of T-ALL patients. All of these genes were upregulated in the T-ALL samples compared to their levels in control samples. HGF, a member of the peptidase S1 family of serine proteases, is associated with cell growth, cell motility and morphogenesis in numerous cell and tissue types [43]. Aberrant functioning of IL2RA and IL10 is associated with many types of cancers [44]. P2RY1 and KALRN have some connections with the nervous system [45]. PF4 and PPBP, which are chemokine family members, interact with PIK3CB and participate in the formation and development of cancer [46]. QRFP encodes a preproprotein that is proteolytically processed to generate multiple protein products. These products are members of the RFamide family of neuropeptides and may play roles in the regulation of blood pressure, reproduction and food intake [47]. Targeting of SCCPDH has been proved as a new cellular target for cancer therapeutics [48]. The present results suggest that HGF, IL2RA, IL10, KALRN, P2RY1, PF4, PIK3CB, PPBP, QRFP, and SCCPDH are potential markers for the treatment of T-ALL.

5. Conclusions

In summary, we investigated the gene expression profile of mRNA sequences from T-ALL mice and constructed seven disease clusters based on the 1475 DEGs. Several T-ALL-associated signaling pathways, such as the PI3K/Akt and FoxO signaling pathways, were identified by enrichment analysis. Survival analysis revealed ten DEGs significantly associated with the survival rates of T-ALL mice that are potential early diagnostic markers for T-ALL and therapeutic targets.

Contributions

Chunlan Hua carried out the conception, design and performed the experiments, analyzed the data, drafting of the article; Xiangyu Chen

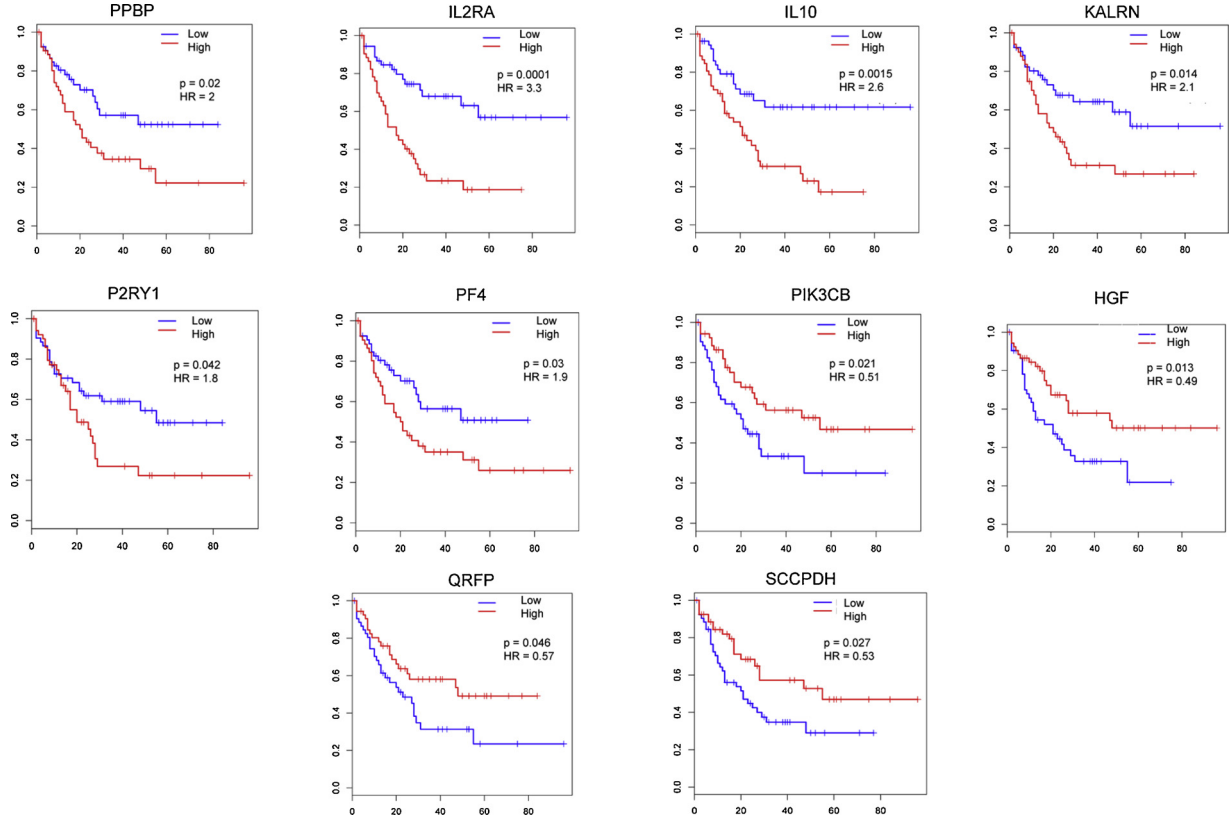

Fig. 4. The present results demonstrated that the expression of HGF, PIK3CB, QRFP and SCCPDH in T-ALL samples is negatively associated with the survival rates of T-ALL mice. However, the expression of PPBP, IL2RA, IL10, KALRN, P2YRY1, and PF4 is positively associated with the survival rates of T-ALL mice. Blue and red curves indicate samples with lower and higher expression levels than median expression levels, respectively. (For interpretation of the references to colour in this figure legend, the reader is referred to the web version of this article).

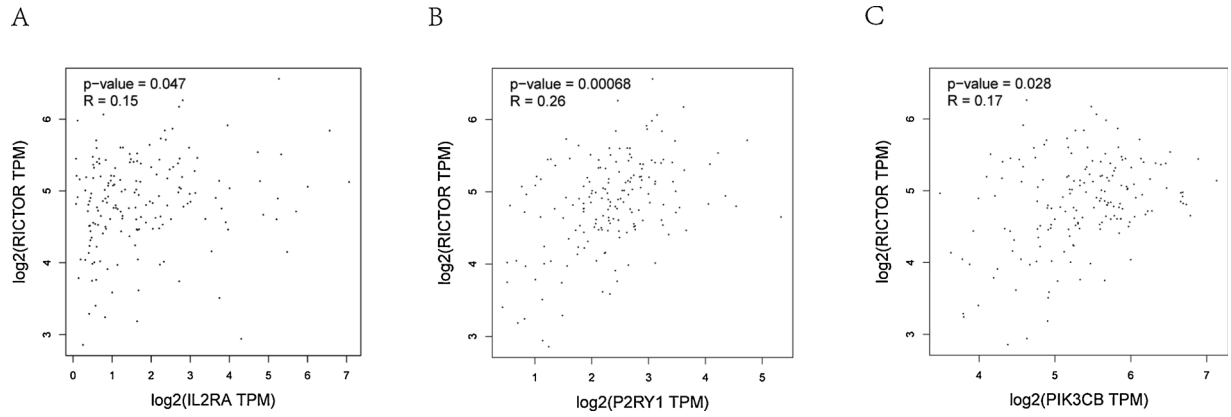

Fig. 5. Correlation analyses were performed to identify the associations of Rictor and the 10 DEGs (pearson correlation coefficient (r) and p value). Three genes, IL2RA, P2RY1 and PIK3CB, are closely related to Rictor ($p < 0.05$).

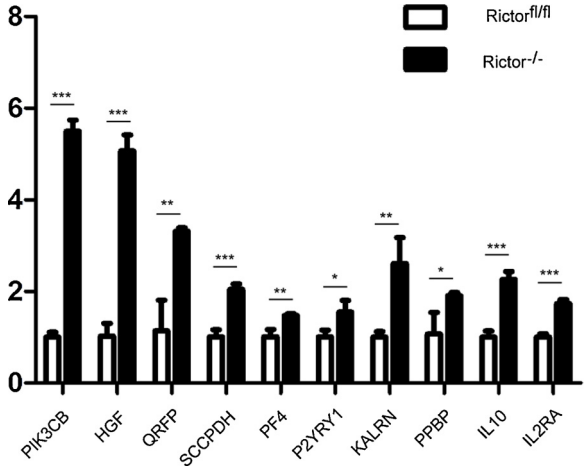

Fig. 6. Validation of the data with RT-PCR. The ten genes identified in RNA-seq data were validated by RT-PCR. *P < 0.01, ***P < 0.001.

and Weiping Yuan, performed research experiments, edited the language; Yang Li performed data analysis and interpretation; Haijun Li and Jing Yu provided critical revisions; Liang Ming contributed to the concept and design, provided drafting of the article, gave final approval and obtained funding. All authors read and approved the final manuscript.

Declaration of Competing Interest

No financial interests/relationships with financial interests related to the topic of this article have been declared.

Acknowledgement

This work was supported by the Youth Foundation of the First Affiliated Hospital of Zhengzhou University.

References

[1] K. Lee, K.T. Nam, S.H. Cho, et al., Vital roles of mTOR complex 2 in Notch-driven thymocyte differentiation and leukemia, J. Exp. Med. 209 (4) (2012) 713–728.
[2] C. Hua, H. Guo, J. Bu, et al., Rictor/mammalian target of rapamycin 2 regulates the development of notch1 induced murine T-ALL via FoxO3a, Exp. Hematol. 42 (12) (2014) 1031–1040.
[3] Y. Zhang, C. Hua, H. Cheng, et al., Distinct sensitivity of $CD8^+CD4^-$ and $CD8^+CD4^+$ leukemic cell subpopulations to cyclophosphamide and rapamycin in Notch1-induced T-ALL mouse model, Leuk. Res. 37 (11) (2013) 1592–1601.
[4] C.H. Pui, J.T. Sandlund, D. Pei, et al., Improved outcome for children with acute lymphoblastic leukemia results of Total Therapy Study XIIIB at St Jude Children's Research Hospital, Blood 104 (9) (2004) 2690–2696.
[5] J.M. Goldberg, L.B. Silverman, D.E. Levy, et al., Childhood T-cell acute lymphoblastic leukemia the Dana-Farber Cancer Institute acute lymphoblastic leukemia consortium experience, J. Clin. Oncol. 21 (19) (2003) 3616–3622.
[6] E. Thiel, B.R. Kranz, A. Raghavachar, et al., Prethymic phenotype and genotype of pre-T ($CD7^+ER^-$)-cell leukemia and its clinical significance within adult acute lymphoblastic leukemia, Blood. 73 (5) (1989) 1247–1258.
[7] D.M. Sabatini, mTOR and cancer insights into a complex relationship, Nat. Rev. Cancer 6 (9) (2006) 729–734.
[8] V.S. Rodrik-Outmezguine, S. Chandarlapaty, N.C. Pagano, et al., mTOR kinase inhibition causes feedback-dependent biphasic regulation of AKT signaling, Cancer Discov. 1 (2011) 248–259.
[9] D. Kalaitzidis, S.M. Sykes, Z. Wang, et al., mTOR complex 1 plays critical roles in hematopoiesis and Pten-loss-evoked leukemogenesis, Cell Stem Cell 11 (3) (2012) 429–439.
[10] T. Hoshii, A. Kasada, T. Hatakeyama, et al., Loss of mTOR complex 1 induces developmental blockage in early T-lymphopoiesis and eradicates T-cell acute lymphoblastic leukemia cells, Proc. Natl. Acad. Sci. U. S. A. 111 (10) (2014) 3805–3810.
[11] G. Distefano, M. Boca, I. Rowe, et al., Polycystin-1 regulates extracellular signal-regulated kinase-dependent phosphorylation of tuberin to control cell size through mTOR and its downstream effectors S6K and 4EBP1, Mol. Cell. Biol. 29 (9) (2009) 2359–2371.
[12] E.K. Han, J.D. Leverson, T. McGonigal, et al., Akt inhibitor A-443654 induces rapid Akt Ser473 phosphorylation independent of mTORC1 inhibition, Oncogene 26 (38) (2007) 5655–5661.
[13] D.D. Sarbassov, D.A. Guertin, S.M. Ali, et al., Phosphorylation and regulation of Akt/PKB by the Rictor-mTOR complex, Science 307 (5712) (2005) 1098–1101.
[14] B.D. Manning, A. Toker, AKT/PKB signaling navigating downstream, Cell. 169 (3) (2017) 381–405.
[15] S.A. Armstrong, A.T. Look, Molecular genetics of acute lymphoblastic leukemia, J. Clin. Oncol. 23 (26) (2005) 6306–6315.
[16] M.B. Mansur, M. Emerenciano, A. Splendore, et al., T-cell lymphoblastic leukemia in early childhood presents NOTCH1 mutations and MLL rearrangements, Leuk. Res. 34 (April (4)) (2010) 483–486.
[17] A.A. Ferrando, D.S. Neuberg, J. Staunton, et al., Gene expression signatures define novel oncogenic pathways in T cell acute lymphoblastic leukemia, Cancer Cell 1 (1) (2002) 75–87.
[18] C. Zhang, Y.K. Ryu, T.Z. Chen, et al., Synergistic activity of rapamycin and dexamethasone in vitro and in vivo in acute lymphoblastic leukemia via cell-cycle arrest and apoptosis, Leuk. Res. 36 (3) (2012) 342–349.
[19] V.I. Brown, A.E. Seif, G.S. Reid, et al., Novel molecular and cellulartherapeuti targets in acute lymphoblastic leukemia and lymphoproliferative, Immunol. Res. 42 (1–3) (2008) 84–105.
[20] C. Evangelisti, F. Ricci, P. Tazzari, et al., Targeted inhibition of mTORC1 and mTORC2 by active-site mTOR inhibitors has cytotoxic effects in T-cell acute lymphoblastic leukemia, Leukemia 25 (5) (2011) 781–791.
[21] X. Li, H. von Boehmer, Notch signaling in T-Cell development and T-ALL, ISRN Hematol. 2011 (2011) 921706.
[22] C. Trapnell, A. Roberts, L. Goff, et al., Differential gene and transcript expression analysis of RNA-seq experiments with TopHat and Cufflinks, Nat. Protoc. 7 (3) (2012) 562–578.
[23] W. Huang da, B.T. Sherman, R.A. Lempicki, Systematic and integrative analysis of large gene lists using DAVID bioinformatics resources, Nat. Protoc. 4 (1) (2009) 44–57.
[24] A. Subramanian, P. Tamayo, V.K. Mootha, et al., Gene set enrichment analysis a knowledge-based approach for interpreting genome-wide expression profiles, Proc. Natl. Acad. Sci. U. S. A. 102 (43) (2005) 15545–15550.
[25] H. Peng, S. Wang, L. Pang, et al., Comprehensive bioinformation analysis of methylated and differentially expressed genes in esophageal squamous cell carcinoma, Mol. Omics 15 (1) (2019) 88–100.
[26] S. Smita, A. Katiyar, D.M. Pandey, et al., Identification of conserved drought stress

responsive gene-network across tissues and developmental stages in rice, Bioinformation 9 (2) (2013) 72–78.
[27] X. Yin, J. Sun, H. Zhang, et al., Comprehensive analysis of multi Ewing sarcoma microarray datasets identifies several prognosis biomarkers, Mol. Med. Rep. 18 (5) (2018) 4229–4238.
[28] C. Xie, X. Mao, J. Huang, et al., KOBAS 2.0 A web server for annotation and identification of enriched pathways and diseases, Nucleic Acids Res. 39 (Web Server issue) (2011) 316–322.
[29] B. Szarzyńska-Zawadzka, M. Dawidowska, T-cell acute lymphoblastic leukemia from miRNA perspective Basic concepts, experimental approaches, and potential biomarkers, Blood Rev. 32 (6) (2018) 457–472.
[30] Y. Ono, N. Fukuhara, O. Yoshie, TAL1 and LIM-only proteins synergistically induce retinaldehyde dehydrogenase 2 expression in T-cell acute lymphoblastic leukemia by acting as cofactors for GATA3, Mol. Cell. Biol. 18 (12) (1998) 6939–6950.
[31] J. O'Neil, A.T. Look, Mechanisms of transcription factor deregulation in lymphoid cell transformation, Oncogene 26 (47) (2007) 6838–6849.
[32] C.H. Pui, D. Pei, D. Campana, et al., Improved prognosis for older adolescents with acute lymphoblastic leukemia, J. Clin. Oncol. 29 (4) (2011) 386–391.
[33] W. Guo, S. Schubbert, J.Y. Chen, et al., Suppression of leukemia development caused by PTEN loss, Proc. Natl. Acad. Sci. U. S. A. 108 (4) (2011) 1409–1414.
[34] J.E. Dick, Looking ahead in cancer stem cell research, Nat. Biotechnol. 27 (1) (2009) 44–46.
[35] L. Zhao, P.K. Vogt, Hot spot mutations in p110alpha of phosphatidylinositol 3 kinase (pI3K) differential interactions with the regulatory subunit p85 and with RAS, Cell Cycle 9 (3) (2010) 596–600.
[36] M.R. Janes, J.J. Limon, L. So, et al., Effective and selective targeting of leukemia cells using a TORC1/2 kinase inhibitor, Nat. Med. 16 (2) (2010) 205–213.
[37] Y. Zhang, T. Hu, C. Hua, et al., Rictor is required for early B cell development in bone marrow, PLoS One 9 (8) (2014) e103970.
[38] F. Chiarini, C. Grimaldi, F. Ricci, et al., NVP-BEZ235 against T-Cell acute lymphoblastic leukemia 3-KinaseMammalian target of rapamycin inhibitor activity of the novel dual phosphatidylinositol, Cancer Res. 70 (20) (2010) 8097–8107.
[39] M. Breuleux, M. Klopfenstein, C. Stephan, et al., Increased AKT S473 phosphorylation after mTORC1 inhibition is Rictor dependent and does not predict tumor cell response to PI3K/mTOR inhibition, Mol. Cancer Ther. 8 (4) (2009) 742–753.
[40] N. Chapuis, S. Park, L. Leotoing, et al., IkB kinase overcomes PI3K/Akt and ERK/MAPK to control FOXO3a activity in acute myeloid leukemia, Blood 116 (20) (2010) 4240–4250.
[41] D. Lee, S.M. Sykes, D. Kalaitzidis, et al., Transmembrane inhibitor of RICTOR/mTORC2 in hematopoietic progenitors, Stem Cell Rep. 3 (5) (2014) 832–840.
[42] F. Pellicano, M.T. Scott, G. Vignir Helgason, et al., The antiproliferative activity of kinase inhibitors in chronic myeloid leukemia cells is mediated by FOXO transcription factors, Stem Cells 32 (9) (2014) 2324–2337.
[43] R. Zhen, J. Yang, Y. Wang, et al., Hepatocyte growth factor improves bone regeneration via the bone morphogenetic protein 2 mediated NF κB signaling pathway, Mol. Med. Rep. 17 (4) (2018) 6045–6053.
[44] C.I. Kobayashi, K. Takubo, H. Kobayashi, et al., The IL-2/CD25 axis maintains distinct subsets of chronic myeloid leukemia-initiating cells, Blood 123 (16) (2014) 2540–2549.
[45] A. Delekate, M. Füchtemeier, T. Schumacher, et al., Metabotropic P2Y1 receptor signalling mediates astrocytic hyperactivity in vivo in an Alzheimer's disease mouse model, Nat. Commun. 5 (2014) 5422.
[46] T. Kuroishi, K. Bando, Y. Tanaka, et al., CXCL4 is a novel nickel-binding protein and augments nickel allergy, Clin. Exp. Allergy 47 (8) (2017) 1069–1078.
[47] C. Jossart, M. Mulumba, R. Granata, et al., Pyroglutamylated RF-amide peptide (QRFP) gene is regulated by metabolic endotoxemia, Mol. Endocrinol. 28 (1) (2014) 65–79.
[48] B. Zheng, H. Guo, N. Ma, et al., Cell- and tissue-based proteome profiling and bioimaging with probes derived from a potent AXL kinase inhibitor, Chem. Asian J. 13 (18) (2018) 2601–2605.